

RESEARCH ARTICLE



## Jing-an oral liquid alleviates Tourette syndrome via the NMDAR/MAPK/CREB pathway *in vivo* and *in vitro*

Leying Xi<sup>a,b</sup>, Xixi Ji<sup>a,b</sup>, Wenxiu Ji<sup>a,b</sup>, Yue'e Yang<sup>a</sup>, Yajie Zhang<sup>c,d</sup> and Hongyan Long<sup>a,b,c,d</sup>

<sup>a</sup>Department of Pediatrics, Nanjing Hospital of Chinese Medicine Affiliated to Nanjing University of Chinese Medicine, Nanjing, China;

<sup>b</sup>Department of Pediatric, Nanjing University of Chinese Medicine, Nanjing, China; <sup>c</sup>Central Laboratory, Nanjing Hospital of Chinese Medicine

Affiliated to Nanjing University of Chinese Medicine, Nanjing, China; <sup>d</sup>Clinical Biobank of Nanjing Hospital of Chinese Medicine, Nanjing Hospital of Chinese Medicine, Nanjing University of Chinese Medicine, Nanjing, China

### ABSTRACT

**Context:** Jing-an oral liquid (JA) is a Chinese herbal formula used in the treatment of Tourette syndrome (TS); however, its mechanism is unclear.

**Objective:** To investigate the effects of JA on amino acid neurotransmitters and microglia activation *in vivo* and *in vitro*.

**Materials and methods:** Sixty male Sprague–Dawley rats were divided into a control group and 5 TS groups. TS was induced in rats with intraperitoneal injection of 1-(2,5-dimethoxy-4-iodophenyl)-2-amino-propane (1 mg/kg) and in BV2 cells with lipopolysaccharide. Control and model rats were administered saline, whereas treatment groups were administered JA (5.18, 10.36, or 20.72 g/kg) or tiapride (a benzamide, 23.5 mg/kg) by gavage once daily for 21 days. Stereotypic behaviour was tested. The levels of *N*-methyl-D-aspartate receptor (NMDAR)/mitogen-activated protein kinase/cAMP response element-binding protein (CREB)-related proteins in striatum and BV2 cells were measured via western blots. CD11b and Iba1 levels were also measured. Ultra-high-performance liquid-chromatography was used to determine  $\gamma$ -aminobutyric acid (GABA), glutamic acid (Glu), and aspartic acid (ASP) levels.

**Results:** JA markedly alleviated the stereotypic behaviour ( $25.92 \pm 0.35$  to  $13.78 \pm 0.47$ ) in rats. It also increased NMDAR1 ( $0.48 \pm 0.09$  to  $0.67 \pm 0.08$ ;  $0.54 \pm 0.07$  to  $1.19 \pm 0.18$ ) expression and down-regulated the expression of p-ERK, p-JNK, p-P38, and p-CREB in BV2 cells and rat striatum. Additionally, Glu, ASP, GABA, CD11b, and Iba1 levels were significantly decreased by JA.

**Discussion and conclusions:** JA suppressed microglia activation and regulated the levels of amino acid neurotransmitters, indicating that it could be a promising therapeutic agent for TS.

### ARTICLE HISTORY

Received 8 February 2022

Revised 1 July 2022

Accepted 13 August 2022

### KEYWORDS





Amino acid neurotransmitters; microglia; *N*-methyl-D-aspartate receptor


### Introduction

Tourette syndrome (TS) is the most common mental and motor disorder in children. Its clinical manifestations are multiple motor and phonic tics, often accompanied by attention deficit hyperactivity disorder, mood disorder, and obsessive-compulsive disorder (OCD), some of which can continue into adulthood (Szejko et al. 2020). Studies have shown that the incidence of TS is 0.4–3.8% internationally and this rate increases annually (Robertson 2008a, 2008b). For the treatment of TS, the first preference should be given to psychoeducation and to behavioural approaches. The pharmacological interventions include aripiprazole, haloperidol, tiapride, clonidine, and guanfacine. The aetiology and pathogenesis of TS are complex and still unclear. There has been an increasing interest in neurotransmitter imbalance in current research. It has been reported that TS is associated with an imbalance in the levels of amino acid neurotransmitters in the cortico-striato-thalamo-cortex (CSTC) loop (Albin and Mink 2006). For example, the levels of glutamate (Glu) and  $\gamma$ -aminobutyric acid (GABA) in the CSTC loop

were increased and related to improved selective motor inhibition in children with TS in a previous study (Mahone et al. 2018). Additionally, it has been shown that Glu release in the CSTC loop is directly associated with tic disorder behaviour in D1CT-7 mice (TS transgenic model) (O'Brien et al. 2018).

Microglia are innate immune effector cells in the brain that play a crucial role in physiological processes in the central nervous system (CNS) (Arcuri et al. 2017). It has been found that there is a correlation between the state of microglia and the occurrence of TS. Moreover, it has been reported that the expression of microglia transporter proteins in the bilateral caudate nucleus is increased in children with TS (Kumar et al. 2015). Additionally, an analysis of the autopsy reports for TS patients reveals an increased number of CD45<sup>+</sup> expressing microglia cells in striatal areas of the basal ganglia (Lenington et al. 2016). Over-activated microglia cells produce reactive oxygen species, inflammatory cytokines, chemokines, and Glu (Takeuchi and Suzumura 2014). The release of excitatory amino acids by microglia is a key mediator of excitotoxic damage. Microglia cells

**CONTACT** Hongyan Long  [longhongyan@njucm.edu.cn](mailto:longhongyan@njucm.edu.cn)  Department of Pediatrics, Nanjing Hospital of Chinese Medicine Affiliated to Nanjing University of Chinese Medicine, Nanjing, Jiangsu, China; Yajie Zhang  [zhangyajie@njucm.edu.cn](mailto:zhangyajie@njucm.edu.cn)  Department of Central Laboratory, Nanjing Hospital of Chinese Medicine Affiliated to Nanjing University of Chinese Medicine, Nanjing, Jiangsu, China

 Supplemental data for this article can be accessed on the publisher's website at <http://dx.doi.org/10.1080/13880209.2022.2116056>.

© 2022 The Author(s). Published by Informa UK Limited, trading as Taylor & Francis Group.

This is an Open Access article distributed under the terms of the Creative Commons Attribution-NonCommercial License (<http://creativecommons.org/licenses/by-nc/4.0/>), which permits unrestricted non-commercial use, distribution, and reproduction in any medium, provided the original work is properly cited.

express various Glu receptors (GluRs); however, the N-methyl-D-aspartate receptor (NMDAR) is crucial for the activity of Glu. Unfortunately, the relationship between NMDAR and signaling mechanisms in TS is unknown. Recent evidence suggests that mitogen-activated protein kinase (MAPK) plays a critical role in regulating the neurochemical and pathophysiological properties of NMDAR (Haddad 2005). As one of the downstream targets of MAPK signaling, cyclic AMP response element-binding protein (CREB) can be phosphorylated. Moreover, MAPK signaling, in the presence of excitatory neurotransmitters and stress is involved in the development of CNS diseases (Koga et al. 2019).

Jing-an Oral Liquid (JA) is a Chinese herbal formulation consisting of eight herbs: *Rehmannia glutinosa* Libosch. (Scrophulariaceae), *Bombyx mori* Linnaeus. (infected with *Beauveria bassiana* Bals.) (Bombycidae), *Paeonia lactiflora* Pall. (Ranunculaceae), *Gastrodia elata* Bl. (Orchidaceae), *Curcuma wenyujin* Y.H.Chen et C.Ling (Zingiberaceae), *Pheretima aspergillum* E.Perrier (Megascolecidae), *Uncaria rhynchophylla* (Miq.) Miq. Ex Havil. (Rubiaceae), and *Buthus martensii* Karsch (Buthidae). Children with TS in China have been clinically treated with JA for many years. JA was formulated based on the compatibility theory of herbal formulation in traditional Chinese medicine, it can nourish Shen Yin, settle Liver Wind, resolve phlegm, and calm the mind. However, the mechanism underlying the beneficial effects of JA in TS children is unknown.

In the present study, we investigated the effects of JA on 1-(2,5-dimethoxy-4-iodophenyl)-2-aminopropane (DOI)-induced TS in rat as well as in lipopolysaccharide (LPS)-treated BV2 microglia cells. The levels of several amino acid neurotransmitters in the BV2 cells and the brain tissues of the rats were investigated. Additionally, the activation level of microglia was evaluated to explore the possible biochemical mechanisms underlying the beneficial effects of JA in TS *in vivo* and *in vitro*.

## Materials and methods

### Drugs and reagents

Tiapride hydrochloride tablets (batch number, H32025477) were purchased from Jiangsu Nwha Pharma. Co., Ltd. (Xuzhou, China). DOI (CAS number, 42203-78-1) and LPS (*Escherichia coli*, 055:B5; EC number, 297-473-0) were obtained from Sigma-Aldrich (St. Louis, MO, USA). Foetal bovine serum (FBS), penicillin/streptomycin, Dulbecco's Modified Eagle Medium/Nutrient Mixture F-12 (F12), and phosphate-buffered saline (PBS) were obtained from Bio-Channel Biotechnology Co., Ltd. (Nanjing, Jiangsu, China) unless otherwise stated. Cell Counting Kit-8 (CCK-8) was obtained from Dojindo Molecular Technologies (Shanghai, China).

### Preparation of JA extract

JA was provided by the Pharmaceutical Department of Nanjing Hospital of Chinese Medicine Affiliated to Nanjing University of Chinese Medicine (Nanjing, China). The formulation contained *Rehmannia glutinosa* (no. 20201014JA-01), *Bombyx mori* (no. 20201014JA-02), *Paeonia lactiflora* (no. 20201014JA-03), *Gastrodia elata* (no. 20201014JA-04), *Curcuma wenyujin* (no. 20201014JA-05), *Pheretima aspergillum* (no.20201014JA-06), *Uncaria rhynchophylla* (no. 20201014JA-07), and *Buthus martensii* (no. 20201014JA-08) at a ratio of 12:9:9:9:9:6:3. The total weight of the herbs was 66 g. The Latin names of the herbs were obtained from the Chinese Pharmacopoeia (2015). Voucher

specimens are stored at the Central Laboratory of Nanjing Hospital. The eight herbs were soaked 10 times in pure water for 30 min, after which extraction was performed at 100 °C for 2 h. The JA solution prepared was then concentrated to obtain a 1.5 g/mL extract.

### Analysis of the main constituents in JA extract by ultra high-performance liquid-chromatography (UHPLC)-tandem mass spectrometry (MS/MS)

The main components of the JA formulation were identified by UHPLC-MS/MS. Chromatographic separation was performed using 1290 Infinity High-Performance Liquid Chromatography system (Agilent Technologies, Inc., Santa Clara, CA, USA). The sample was separated on an Agilent ZORBAX Eclipse Plus C18 column (2.1 × 50 mm, 1.8 μm) at 30 °C. The mobile phase consisted of methyl alcohol (A) and 0.1% formic acid-acetonitrile (B), and was run at a flow rate of 0.3 mL/min in gradient elution as follows: 0–5 min: 90–65% B; 5–20 min: 65–60% B; 20–25 min: 60–10% B; 25–27 min: 10% B; 27–28 min: 10–90% B; and 28–29 min: 90% B. MS/MS analysis was performed using an Agilent 6460 Triple Quad LC/MS system. The collision voltages of the positive and negative ion sources were 4000 and 3500 V, respectively. The temperature and the flow rate of the drying gas were 350 °C and 10 L/min, respectively.

### Preparation of medicated rat serum

Male Sprague-Dawley rats ( $n=25$ ; weight,  $180 \pm 20$  g) were obtained from Beijing Vital River Laboratory Animal Technology Co., Ltd. (license number, SCXK [Zhe] 2019-0001; Beijing, China) and randomly divided into five groups ( $n=5$  per group) for the study. Three groups were administered JA at a low, medium, or high dose (5.18, 10.36, or 20.72 g/kg, respectively); the doses were named JA-L, JA-M, and JA-H, respectively. One group was administered tiapride hydrochloride (23.5 mg/kg), whereas the last group was administered saline at the same volume once daily for 5 days. All the test formulations were administered intragastrically. Rats were anaesthetized by 1% sodium pentobarbital (40 mg/kg, i.p.). Blood was collected from the abdominal aorta and centrifuged for 15 min (3000 rpm, 4 °C). Serum was sterilized by vacuum filtration and stored at  $-80$  °C. A flow chart of all procedures is shown in [supplementary methods](#).

### Cell culture

BV2 cells were grown in F12 medium supplemented with 10% FBS and 1% penicillin/streptomycin. The culture medium was changed every day. The cells were maintained at 37 °C in a humidified atmosphere containing 95% O<sub>2</sub> and 5% CO<sub>2</sub>.

### Cell viability

BV2 cell viability was assessed using CCK-8 according to the manufacturer's instructions. The cells were seeded in 96-well plates ( $1 \times 10^4$  cells/well). After 24 h of incubation, the cells were treated with different concentrations of LPS (0, 0.1, 0.25, 0.5, 1, 2, or 5 μg/mL) or JA (5, 10, 15, 20, or 30%) for 24 h. Next, 10 μL CCK-8 solution was added into each well and followed by incubation of the plate for 2 h. Optical density was determined at

450 nm using an Epoch microplate spectrophotometer (Bio-Tek Instruments, Winooski, VT, USA).

### Animal study

Male Sprague–Dawley rats ( $n = 60$ ; weight,  $180 \pm 20$  g) obtained from Beijing Vital River Laboratory Animal Technology Co., Ltd. were housed under a 12 h day/night cycle at room temperature ( $22^\circ\text{C}$ ) for the study. The rats were randomly divided into control, DOI (model), DOI + tiapride ( $23.5$  mg/kg tiapride), DOI + JA-L ( $5.18$  mg/kg JA) group, DOI + JA-M ( $10.36$  mg/kg JA) group and DOI + JA-H ( $20.72$  mg/kg JA) groups ( $n = 10$  per group). All DOI-treated groups were administered  $1$  mg/kg DOI via intraperitoneal injection. The control group was injected intraperitoneally with normal saline at the same volume for 21 days as indicated in our previous reports. All experimental protocols were approved by the Animal Studies Ethics Committee of Nanjing University of Chinese Medicine (approval number, 202111A005). Rats were anaesthetized by 1% sodium pentobarbital ( $40$  mg/kg, i.p.). The cerebrospinal fluid (CSF) were collected and stored at  $-80^\circ\text{C}$  for UHPLC analysis. After CSF collection, striatum tissues were collected and stored at  $-80^\circ\text{C}$  for western blotting, quantitative polymerase chain reaction (q-PCR), immunofluorescence and immunohistochemical analysis. The sample preparation of rat brain corpus striatum for western blotting and sample collection of cerebrospinal fluid are described in [supplementary methods](#).

### Behavioural tests

Two tests were performed in this experiment: grading of stereotypy and classification of stereotype behaviour. Stereotyped behaviour was evaluated by observing DOI-treated rats as described in our previous study (Long et al. 2019). Evaluation of stereotyped behaviour was based on the following scoring criteria: 0, no stereotyped behaviour; 1, rotational behaviour; 2, excessive up and down movement of the head and neck; 3, excessive head and neck movements plus rotation; 4, lateral head swing and excessive up and down movement of the head. Stereotyped behaviour was classified as follows: mouth and claw movement, self-biting, spinning, head shaking (many swings from left to right and up and down), dance-like movement and licking and biting the cage. The number of occurrences of the above behaviours was recorded during a 1 h observational period, and one point was recorded for each occurrence.

### Western blotting

Western blot analyses were performed with the BV2 cells and striatum tissue excised from the rats. In each instance, the sample was homogenized with radioimmunoprecipitation assay buffer containing phosphatase and protease inhibitors (Beyotime, Shanghai, China). Total protein concentration was quantified using a BCA Protein Assay Kit. Protein samples ( $40$   $\mu\text{g}$ /lane) were separated by 10% sodium dodecyl sulfate-polyacrylamide gel electrophoresis and transferred onto polyvinylidene difluoride membranes. The membranes were blocked with 5% bovine serum albumin (BSA; Solarbio, Beijing, China) for 1 h and then incubated with different primary antibodies at  $4^\circ\text{C}$  overnight. The primary antibodies used were rabbit anti-NMDAR1 (1:1000; Abcam, Cambridge, UK), rabbit anti-CD11b (1:1000, Abcam), rabbit anti-extracellular signal-related kinase (ERK) 1/2 (1:1000;

Cell Signalling Technology [CST], Danvers, MA, USA), rabbit anti-phospho-ERK1/2 (1:1000, CST), rabbit anti-JNK (1:1000, CST), rabbit anti-phospho-JNK (1:1000, CST), rabbit anti-P38 (1:1000, CST), rabbit anti-phospho-P38 (1:1000, CST), rabbit anti-CREB (1:1000, Abcam), rabbit anti-phospho-CREB (1:1000, Abcam), and rabbit anti-GAPDH (1:10000, Abcam). After 5 min of washing in Tris-buffered saline with 0.1% Tween $\text{\textcircled{R}}$  20, the membranes were incubated with goat anti-rabbit immunoglobulin G (1:2000, Abcam) for 1 h at room temperature and analyzed using an Immobilon Western kit (Merck Millipore, Burlington, MA, USA). The bands were analyzed using a chemiluminescence detection system and quantified by densitometry using ImageJ software (National Institutes of Health, Bethesda, MD, USA).

### Quantitative polymerase chain reaction (q-PCR)

Total RNA was extracted from BV2 cells and striatum tissue with TRIzol reagent (Thermo Fisher Scientific, Waltham, MA, USA). RNA purity was determined using a NanoDrop 2000 system (Thermo Fisher Scientific), and cDNA was synthesized using a HiScript III RT SuperMix for qPCR Kit at  $37^\circ\text{C}$  for 15 min. Next, qPCR was performed using SYBR Green kit (Takara, Dalian, China) and an ABI 7500 instrument (Bio-Rad Laboratories, Inc., Hercules, CA, USA). The reaction system was comprised of  $10$   $\mu\text{L}$  of  $2 \times$  ChamQ SYBR qPCR Master Mix,  $6$   $\mu\text{L}$  of template DNA,  $0.8$   $\mu\text{L}$  of forward and reverse primers, and added RNase-free water to a final volume of  $20$   $\mu\text{L}$ . The primers used for the rats were as follows: NMDAR1 forward, AGCGGGTAAACAACAGAACAAAA; NMDAR1 reverse, GAATCGGCCAAAGGGACTGAA; CREB forward, ATTCAT TACAAAGGGCGCAAA; CREB reverse, ATATATGCAAATGG CTGGTCCC; CD11b forward, ACCACTCATTGTGGGCAGC TC; CD11b reverse, CACCGGCTTCATT CATCATGTC; Iba1 forward, TCCGAGGAGACGTTTCAGTTAC; Iba1 reverse, CAG TTGGCTTCTGGTGTTCCTT; GADPH forward, ATCACCATCT TCCAGGAGCGA; and GADPH reverse, AGCCTTCTCCATGG TGGTGGA. The primers used for the BV2 cells were as follows: NMDAR1 forward, GAAAACCTCGACCAACTGTCC; NMDAR1 reverse, GTCGTCCTCGCTTGCAGA; CREB forward, GAGCAG ACAACCAGCAGAGT; CREB reverse, TGGCATGGATACCT GGGCTA; CD11b forward, TCGCTACGTAATTGGGGTGG; CD11b reverse, TAGATGCGATGGTGTGAGC; Iba1 forward, AGCCTGAGGAGATTTCAACAGTT; Iba1 reverse, CCTCAG ACGCTGGTTGTCTT; GADPH forward, GGGTCCCAGCTTAG GTTCATG; and GADPH reverse, AATCCGTTACACCGCAC CTT. The amplification criteria were as follows: pre-deformation:  $95^\circ\text{C}$ , 30 s, 1 Rep; and PCR reaction:  $95^\circ\text{C}$ , 4 s,  $60^\circ\text{C}$ , 34 s, 40 Reps. Gene expression was normalized to that of the housekeeping gene GAPDH.

### Immunofluorescence analysis of striatum tissue

NMDAR, p-CREB, and CD11b expression in the striatum was evaluated by immunofluorescence. Briefly, the brain tissue was frozen and the mid-part of the striatum was cut into  $20$   $\mu\text{m}$  slices in the coronal plane. The slices were washed three-times in PBS (pH 7.4) for 5 min each time, blocked with 10% goat serum, and incubated with the following primary antibodies overnight at  $4^\circ\text{C}$ : anti-phospho-CREB (1:1000, Abcam), NMDAR (1:1000, Abcam), and CD11b (1:1000, Abcam). The slices were then incubated with goat anti-rabbit secondary antibody (1:500, Beyotime) for 2 h in the darkness at room temperature, and washed three-

times in PBS for 10 min each time. Images were captured using a fluorescence microscope (IX71; Olympus Corporation, Tokyo, Japan).

### Immunohistochemical analysis

IBa1, p-P38, p-ERK, p-JNK, and p-CREB expression in the striatum tissue were evaluated by immunohistochemistry. The tissues were first embedded in paraffin, sliced dewaxed in xylene, and soaked in 3% hydrogen peroxide. Next, the tissues were blocked with 5% BSA and incubated with the corresponding primary antibody at 4 °C overnight. The samples were then incubated with the corresponding secondary antibody for 1 h at room temperature, stained with diaminobenzidine (Solarbio) for 5 min, and observed under a fluorescence microscope.

### Assay of amino acid neurotransmitters

The levels of amino acid neurotransmitters in CSF and BV2 cells were measured in this test. Briefly, 160  $\mu$ L/500  $\mu$ L of extraction solution (acetonitrile: methanol: water, 2:2:1) was added to the samples, after which the samples were vortexed for 30 s and sonicated in an ice water bath for 15 min. The samples were then incubated at -40 °C for 1 h and centrifuged at 12,000 rpm for 15 min at 4 °C. Next, 80  $\mu$ L of each supernatant was transferred into separate auto-sampler vials for UHPLC/MS/MS analysis. The UHPLC analysis was carried out using an Agilent 1290 Infinity II UHPLC System (Agilent Technologies, Inc.), equipped with a Waters ACQUITY UPLC BEH Amide column (100  $\times$  2.1 mm, 1.7  $\mu$ m). The mobile phase was comprised of 1% formic acid in water (A) and 1% formic acid in acetonitrile (B). The column temperature was set at 35 °C. The auto-sampler temperature was set at 4 °C and the injection volume was 1  $\mu$ L. An Agilent 6460 Triple Quadrupole Mass Spectrometer (Agilent Technologies, Inc.), equipped with an Agilent Jet Stream Electrospray Ionization interface was used for the assay. The ion source parameters were as follows: capillary voltage, +4000/-3500 V; nozzle voltage, +500/-500 V; gas (nitrogen, N<sub>2</sub>) temperature, 300 °C; gas (N<sub>2</sub>) flow rate, 5 L/min; sheath gas (N<sub>2</sub>) temperature, 250 °C; sheath gas flow rate, 11 L/min; and nebulizer pressure, 45 psi. The Agilent MassHunter Workstation Software (B.08.00, Agilent Technologies, Inc.) was used for multiple-reaction monitoring (MRM) data acquisition and processing.

### Statistical analysis

Data were analyzed using GraphPad Prism (version 8.4.2; GraphPad Software Inc., San Diego, CA, USA). All the data obtained have been presented as mean  $\pm$  standard deviation (SD). Group values were analyzed for a normal distribution. Parametric data that were normally distributed were analyzed using one-way ANOVA. Pairwise comparison used Tukey's test. Meanwhile parametric data that were not normally distributed were analyzed using non-parametric test. The behaviour test scores were analyzed using the Mann-Whitney test. Statistical significance was considered at  $p < 0.05$ .

## Results

### Identification of the major components of JA

The total ion and MRM chromatogram for JA are shown in Figure 1. According to the Chinese Pharmacopoeia (2015), the components identified in JA were: isorhynchophylline, rhynchophylline, gastrodin, catalpol, curcumin, and paeoniflorin (Figure 1). The concentrations of the components are listed in Table 1.

### Effects of JA on the behaviour of rats with TS

Stereotypy score was higher in the group with TS than in the control group. The results showed that stereotype score decreased significantly after the rats were treated with tiapride or JA; however, this was not observed in the model group. The classification stereotype behaviour score was higher in the model group than in the control group. Additionally, the score decreased significantly after the rats were treated tiapride or JA (Figure 2).

### Effects of JA on BV2 cell viability

BV2 cells were treated with rat serum containing JA (5, 10, 15, 20, or 30%) for 24 h to confirm that the neuroprotective property of JA is not due to a cytotoxic effect. The BV2 cells were treated with LPS (0, 0.1, 0.25, 0.5, 1, 2, and 5  $\mu$ g/mL) for 24 h. JA did not alter the viability of BV2 cells at the various concentrations tested, suggesting that the neuroprotective property of JA is not as a result of a cytotoxic effect (Figure 3). Therefore, JA was used at a concentration of 10% in the subsequent experiments. Moreover, LPS significantly reduced cell viability at concentrations above 1  $\mu$ g/mL ( $p < 0.05$ ).

### Effects of JA on the NMDAR/MAPK/CREB signaling pathway in BV2 cells and the rat striatum

In order to explore the effect of JA on the NMDAR/MAPK/CREB signaling pathway, we measured the levels of p-ERK1/2, p-JNK, p-P38, p-CREB, and NMDAR1 in the striatum as well as in the LPS-stimulated BV2 cells. As shown in Figure 4, the expression levels of p-ERK1/2, p-JNK, p-P38, and p-CREB increased in the BV2 cells and the striatum tissues of rats in the model group ( $p < 0.05$ ). However, JA decreased the phosphorylation of ERK, JNK, P38, and CREB ( $p < 0.05$ ). Furthermore, NMDAR1 expression was significantly decreased in the TS group but was increased by JA. The effect of JA on microglia activation was also explored in this experiment. The results showed that CD11b expression increased in the TS model group ( $p < 0.05$ ), but was decreased by JA ( $p < 0.05$ ), suggesting that JA inhibit the over activation of microglia.

### Effects of JA on the mRNA levels of NMDAR, CREB, and CD11b in BV2 cells and the rat striatum

The mRNA levels of CREB significantly decreased and the levels of NMDAR1 mRNA significantly increased in the rat striatum as well as in BV2 cells in TS group. Both triapride and JA decreased CREB level and increased NMDAR1 levels ( $p < 0.05$ , Figure 5). These results were consistent with those obtained from the Western blot analysis. Compared to the control group, the model group showed higher mRNA levels of CD11b and IBa1; however, JA decreased the mRNA levels of CD11b and

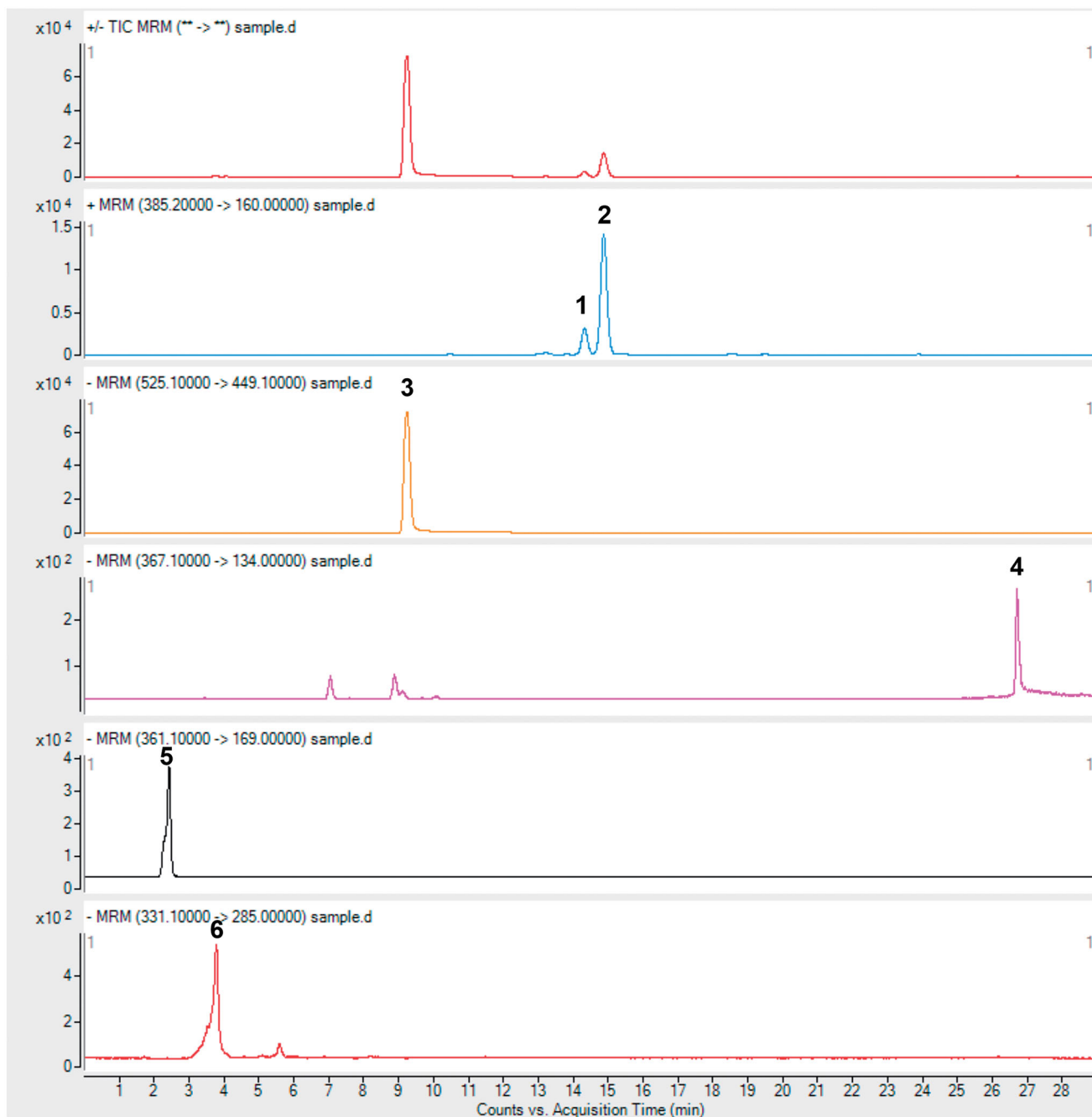


Figure 1. HPLC analysis of JA. Numbers 1–6 represent isorhynchophylline, rhynchophylline, paeoniflorin, curcumin, catalpol, and gastrodin, respectively.

Table 1. Components identified in JA.

Components	Concentration ( $\mu\text{g}/\text{mL}$ )
Isorhynchophylline	2.5
Rhynchophylline	0.8
Gastrodin	20.87
Catalpol	20.3
Curcumin	0.7
Paeoniflorin	1101.8

IBa1 in the BV2 cells as well as in the striatum tissues of rats in the model group ( $p < 0.05$ ). These results suggest that JA can inhibit microglia over activation in TS.

### Immunohistochemical analysis

To further investigate the MAPK/CREB signaling pathway in TS, an immunohistochemical technique was used to measure the expression levels of various related proteins in the rat striatum. Compared to the control group, the model group showed higher expression levels of p-JNK, p-ERK, p-P38, p-CREB, and IBa1 ( $p < 0.05$ ). Additionally, the results showed that JA decreased the levels of p-JNK, p-ERK, p-P38, p-CREB, and IBa1 ( $p < 0.05$ , Figure 6).

### Immunofluorescence analysis

The fluorescence produced by NMDAR1 was weaker whereas that produced by CD11b and p-CREB was stronger in the model

group than in the control group. After the treatment with JA-H, the fluorescence intensity of CD11b and p-CREB decreased, whereas that of NMDAR1 increased (Figure 7). The results suggest that more microglia cells were activated in the TS group compared to the other groups.

### Effect of JA on the levels of amino acid neurotransmitters in rat CSF and BV2 cells

The pathogenesis of TS is closely related to the levels of neurotransmitters; therefore, we measured the levels of GABA, Glu, and ASP in rat CSF and BV2 cells. The levels of Glu and ASP in

CSF were significantly higher in the rats with TS than in the control rats ( $p < 0.05$ ). Moreover, JA-M and JA-H significantly decreased the levels of Glu and ASP ( $p < 0.05$ ), whereas only JA-H decreased the level of ASP ( $p < 0.05$ ) (Figure 8). GABA level did not differ significantly among the groups ( $p > 0.05$ ) (Figure 8(C)). The levels of Glu, ASP, and GABA increased in the LPS-treated BV2 cells; however, only JA-H decreased the levels of these amino acid neurotransmitters ( $p < 0.05$ ). JA-L and JA-M did not alter the levels of Glu, ASP, and GABA ( $p > 0.05$ ) (Figure 8(D)). The lowest detection concentrations of Glu, ASP, and GABA were 8488, 2100, and 2778 nmol/L, respectively, in rat CSF and 6.54, 0.689, and 0.0183 nmol/L, respectively, in BV2 cells.

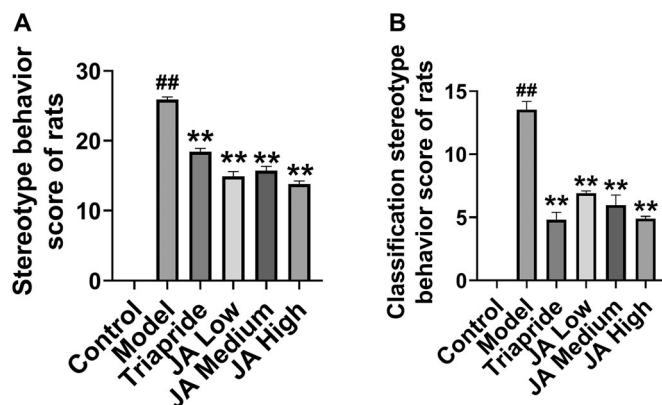


**Figure 2.** Effects of JA on (A) stereotype behaviour and (B) classification stereotype behaviour. Data are presented as mean  $\pm$  SD. ##Indicates  $p < 0.01$  when data are compared to those for the control group. \*\*Indicates  $p < 0.01$  when data are compared to those for the model group. JA Low: JA low dosage (5.18 g/kg); JA Medium: JA medium dosage (10.36 g/kg); JA High: JA high dosage (20.72 g/kg).

### Discussion

In this study, the selective 5-HT<sub>2A/2C</sub> agonist DOI was used to induce TS in rats. The behavioural indicators of TS in rats are more stable and can simulate the behavioural characteristics of TS in humans better than those of other animal models (Ishiguro et al. 2016). Similar to our previous finding, DOI significantly enhanced stereotyped behaviour and classification of stereotyped behaviour associated with TS in the present study (Long et al. 2019a).

The pathogenesis of TS is associated with abnormal levels of excitatory amino acid neurotransmitters such as Glu, ASP, and GABA within the CSTC loop. An increase in the ratio of excitatory to inhibitory amino acids has been proposed to underlie the pathogenesis of neuropsychiatric disorders such as TS, autism spectrum disorder, and OCD (Aida et al. 2015). GABA is the main inhibitory amino acid neurotransmitter, therefore, an imbalance in the Glu/GABA ratio in the CSTC loop can lead to

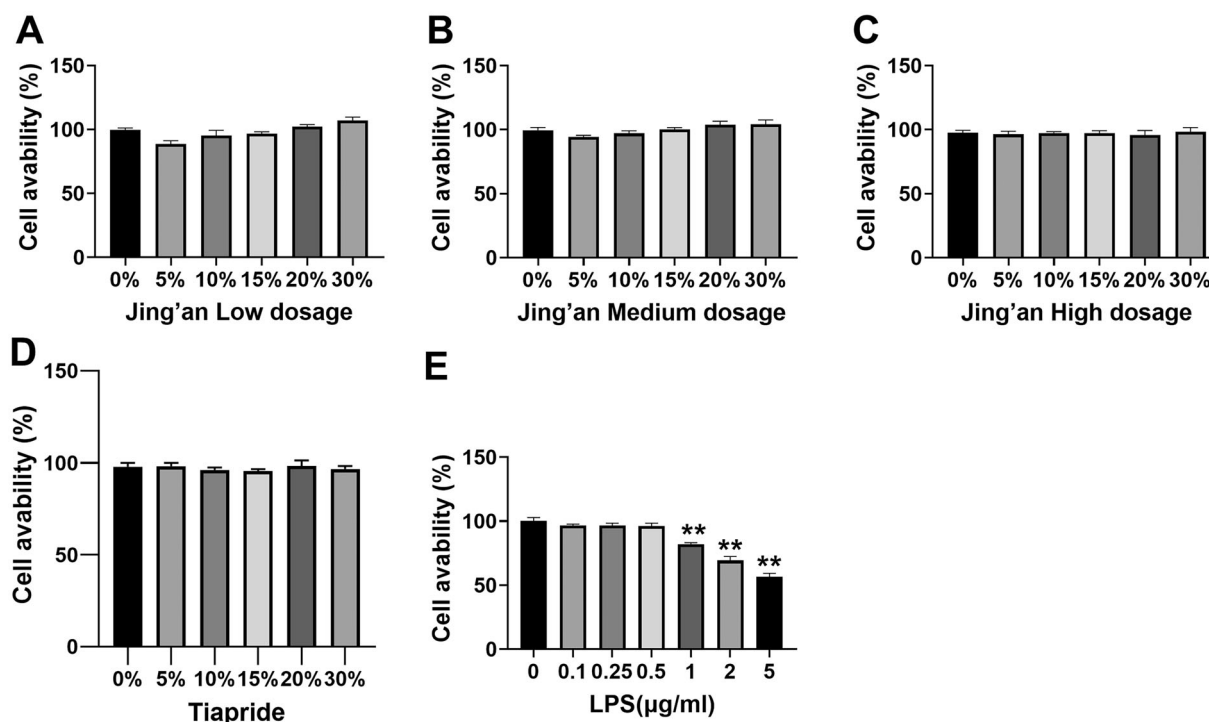


**Figure 3.** Effects of JA-containing and tiapride-containing rat medium on the viability of BV2 cells. (A–D) Viability of the cells. (E) BV2 cells were treated with various concentrations of LPS (0–5  $\mu$ g/ml) for 24 h. Data are presented as mean  $\pm$  SD of the results three independent experiments (\*\*indicates  $p < 0.01$  when data are compared to those for the control). Jing'an Low dosage, medicated rat serum containing JA low dosage (5.18 g/kg); Jing'an Medium dosage, medicated rat serum containing JA medium dosage (10.36 g/kg); Jing'an High dosage, medicated rat serum containing JA high dosage (20.72 g/kg); Tiapride, medicated rat serum containing tiapride (23.5 mg/kg).

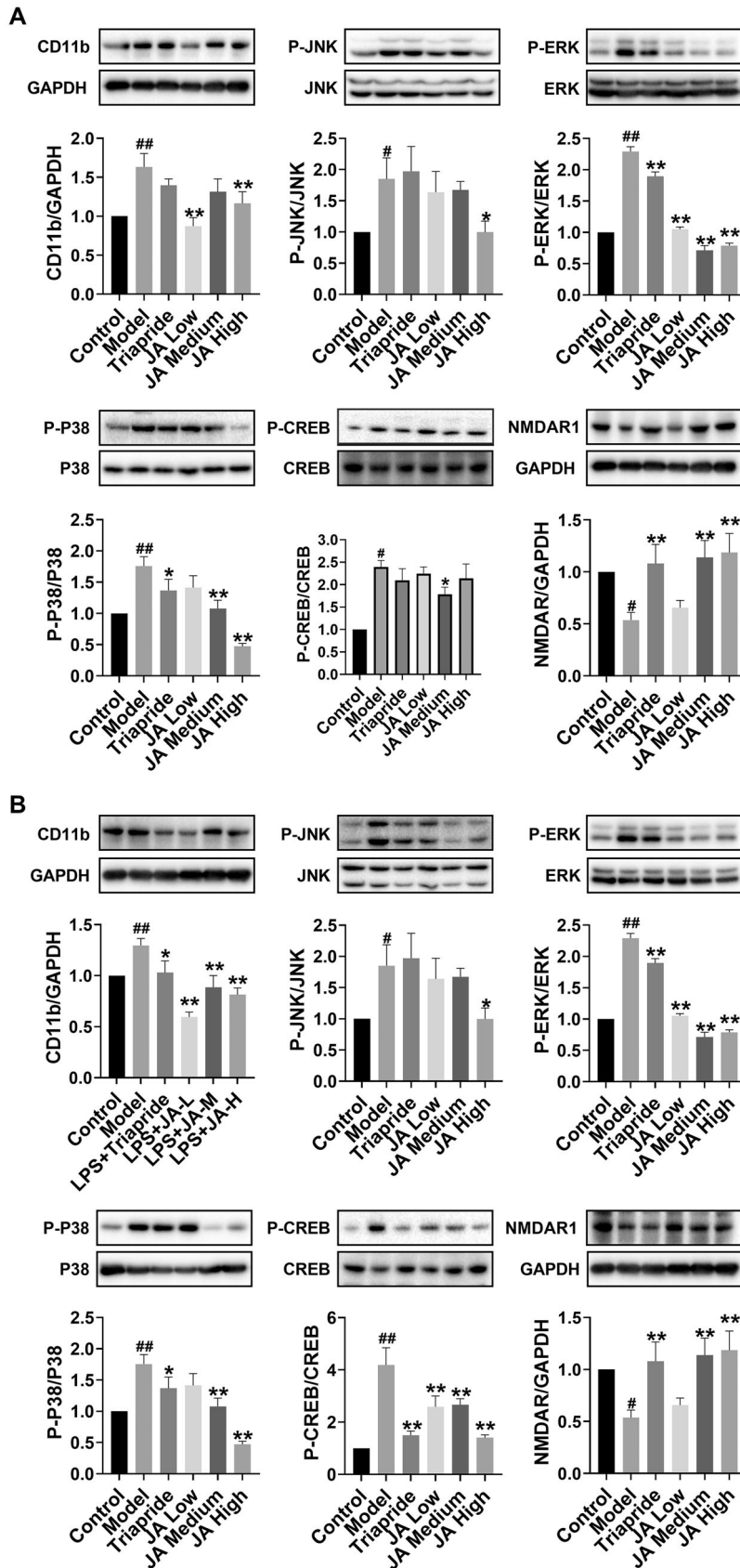


**Figure 4.** Effects of JA on the NMDAR/MAPK/CREB pathway in (A) the rat striatum and (B) BV2 cells. Data are presented as mean  $\pm$  SD. # and ## indicate  $p < 0.05$  and  $p < 0.01$ , respectively, when data are compared to those for the control group. \* and \*\* indicate  $p < 0.05$  and  $p < 0.01$ , respectively, when data are compared to those for the model group.

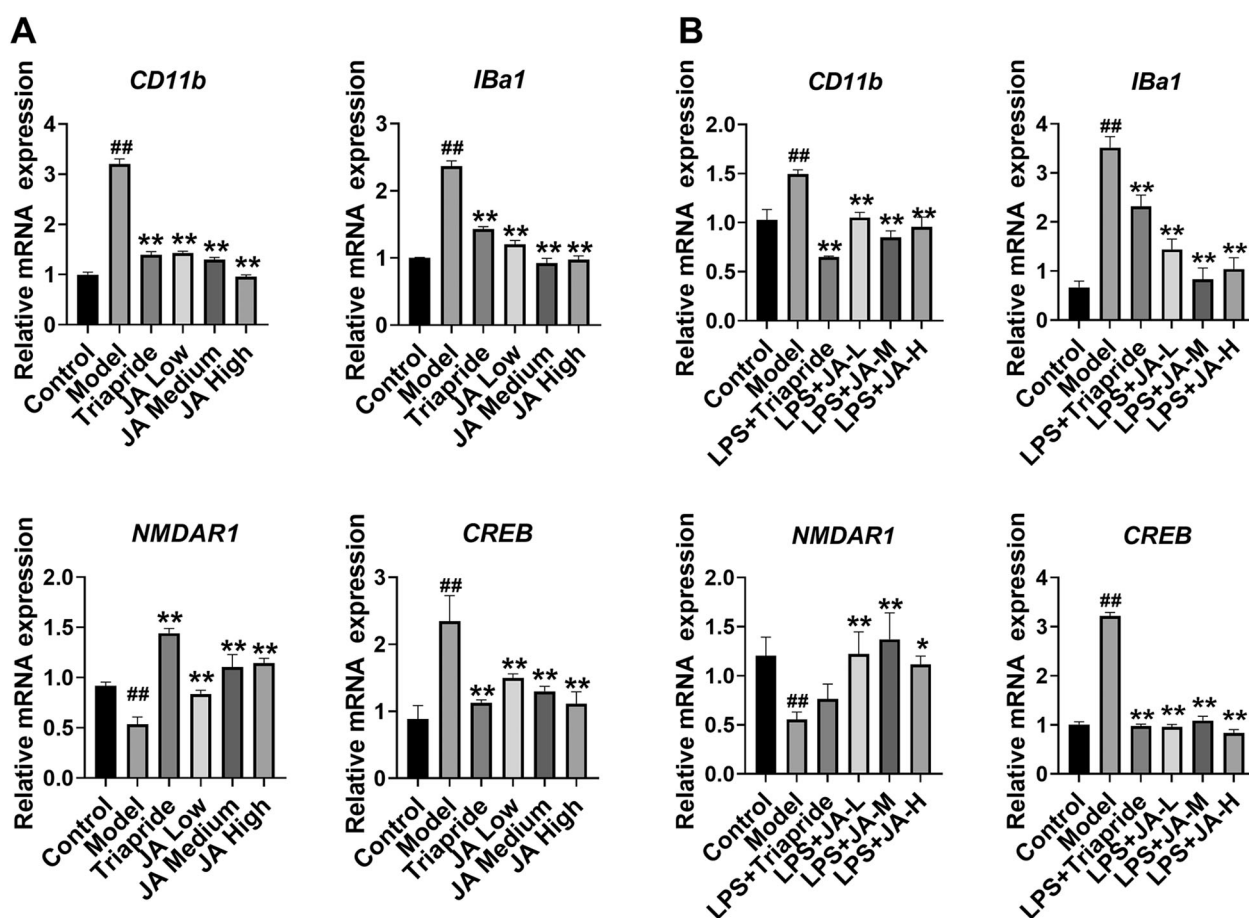


**Figure 5.** Effects of JA on NMDAR/CREB and CD11b levels in (A) the rat striatum and (B) BV2 cells. Data are presented as mean  $\pm$  SD. ##Indicates  $p < 0.01$  when data are compared to those for the control group. \* and \*\*Indicate  $p < 0.05$  and  $p < 0.01$ , respectively, when data are compared to those for the model group.

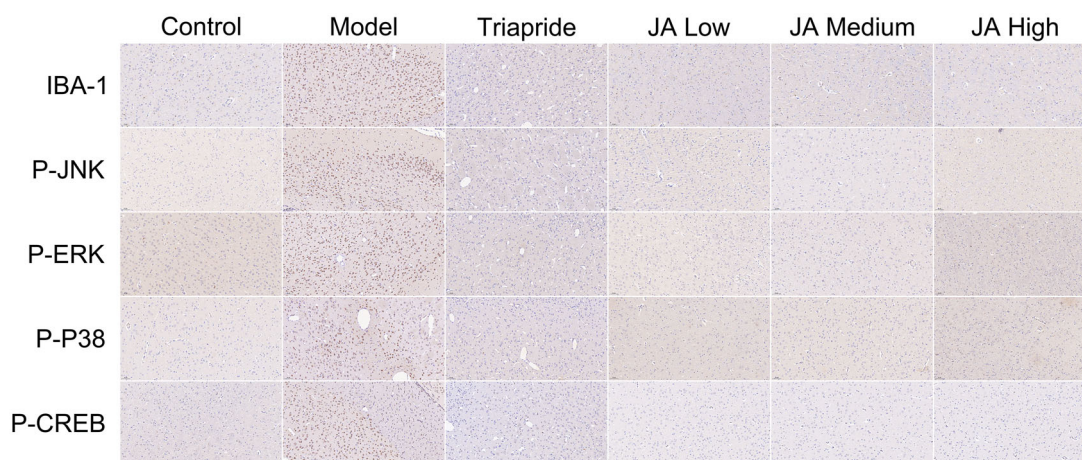


**Figure 6.** Effects of JA on p-JNK, p-ERK, p-p38, p-CREB, and Iba1 levels in the rat striatum. The levels of the various proteins were assessed in an immunohistochemical analysis. Scale bar = 50  $\mu$ m.

tic-like behaviour (Kanaan et al. 2017). However, reports on GABA levels in TS are inconsistent. It has been reported that GABA concentrations in the primary sensorimotor cortex is lower in TS patients than in healthy children (Puts et al. 2015). However, our previous results indicated that the levels of Glu and GABA in striatum were significantly higher in rats with TS than in control rats (Long et al. 2019b). CSF is a colourless and transparent liquid that fills in each cerebral ventricle. When lesions form in the CNS and the metabolism of nerve cells is

disturbed, changes occur in the properties and composition of CSF. However, it is not clear if changes in the levels of amino acid neurotransmitters in the brain are consistent with changes in the levels of amino acid neurotransmitters in the CSF. To clarify this, we evaluated the levels of Glu, ASP, and GABA in both CSF and BV2 cells in this research.

Our results showed that the levels of amino acid neurotransmitters in the CNS differed greatly among the groups. Specially, the levels of Glu and ASP were significantly increased in the



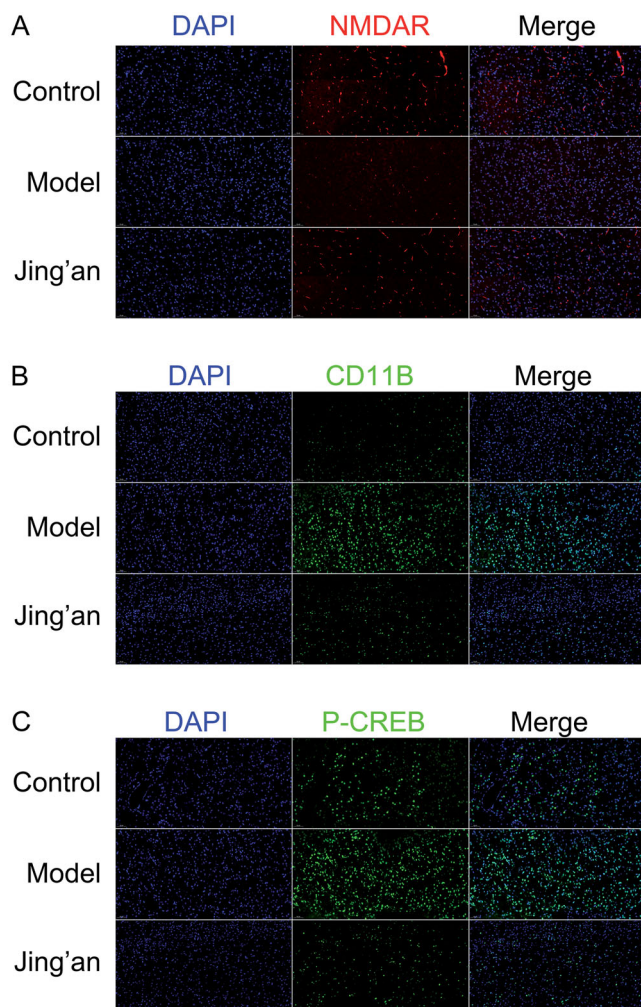


**Figure 7.** Representative image of the immunofluorescence assay performed on striatal tissues. Specimens were stained for (A) NMDAR (red), (B) CD11b (green), (C) p-CREB (green), and (D) 4',6-diamidino-2-phenylindole (blue). Scale bar = 50  $\mu$ m.

CNS of rats with TS. Additionally, JA-M and JA-H significantly decreased the levels of Glu and ASP, whereas JA-L decreased the level of ASP. GABA levels did not differ significantly among the groups. The levels of Glu, ASP, and GABA in BV2 cells were also investigated. The results showed that the levels of these three neurotransmitters increased in the model cells, but were decreased by only JA-H, indicating that similar changes occur in the levels of Glu, ASP, and GABA in CSF and brain tissue in TS. Additionally, there are abnormalities in the levels of these excitatory and inhibitory neurotransmitters in TS. Our results also showed that inhibition of amino acid neurotransmitters was not due to toxicity to microglia, as the various concentrations (5–30%) of JA in the rat serum did not alter the viability of microglia cells.

Microglia are the resident immune cells of the CNS. Abnormally activated microglia secrete high levels of amino acids, which can result in neurological damage. CD11b and Iba1 are the signature proteins of microglia. The binding neurotransmitters to receptors are important for activation downstream signaling pathway. Over the last decade, there has been increasing evidence that microglia can express various functional GluRs, including  $\alpha$ -amino-3-hydroxy-5-methyl-4-isoxazolepropionic acid, kainite, and NMDARs (Murugan et al. 2013). Furthermore, it was

observed in another study that MK801 (a non-competitive NMDAR antagonist) inhibits LPS-induced microglia activation (Thomas and Kuhn 2005). The expression of functional GluRs is evident in microglia, and GluR activation is known to be associated with Glu release, cytokine release, microglia activation, and nitric oxide production (Byrnes et al. 2009; Murugan et al. 2011; Beppu et al. 2013). Therefore, GluRs on microglia may be a therapeutic target for neurological disorders involving microglia activation.

In the present study, we found that the NMDAR/MAPK/CREB pathway is involved in the occurrence of TS. NMDARs are reported to be closely involved in the pathogenesis of TS in the Chinese Han population (Che et al. 2015). Moreover, it has been shown that the levels of NMDAR in the cortex and striatum decreases in rats with TS, but can be increased with treatment of Jian-Pi-Zhi-Dong decoction (Zhang et al. 2020). Similarly, we found that NMDAR level decreased in both the striatum and BV2 cells in the TS model group; however, after the treatment with JA, NMDAR level increased significantly and became higher than in the model group, both *in vitro* and *in vivo*. No direct link has been reported to occur between NMDAR and CREB activation in TS. MAPK signaling pathways that involve ERK1/2, P38 MAPK, and JNK, play important roles in various human diseases. It was found in a previous study that the microglia inactivation induced by ketamine (non-competitive antagonist of NMDAR) may be mediated via inhibition of p-ERK1/2 activity (Chang et al. 2009). In addition, activation of MAPK signaling has been observed in histidine decarboxylase (*Hdc*) knockout mice that exhibit TS-like phenomenology (Rapanelli et al. 2014, 2018). Moreover, MAPK phosphorylates CREB in the presence of excitatory neurotransmitters and is involved in CNS disorders (Koga et al. 2019). There are very limited reports on CREB involvement in TS. It has been reported that p-CREB level does not change in iminodipropionitrile-treated mice but can be increased by a Chinese herbal formulation (Chen et al. 2019). This evidence suggests that the NMDAR/MAPK/CREB pathway may be involved in microglia activation and the production of amino acid neurotransmitters in TS. However, further investigations are required to ascertain whether abnormal levels of amino acid neurotransmitters and microglia hyper-activation occur via the NMDAR/MAPK/CREB pathway. The findings of the present study indicated increased levels of p-JNK, p-ERK, p-P38, and p-CREB in the TS group. Additionally, significant microglia activation and disruption in the levels of amino acid neurotransmitters were observed. It was also found JA inhibited the NMDAR/MAPK/CREB pathway, suppressed microglia activation, and regulated the levels of amino acid neurotransmitters. In the present study, we found tiapride had literally the same effects as JA in alleviating the severity of stereotyped behaviour in rats. While, first, the effects of JA on regulating the levels of amino acid neurotransmitters in BV2 cells and CSF of rats are more stable than that of tiapride. JA was effective both in the microglia cell model (BV2) and CSF, tiapride only regulated the levels of neurotransmitters in CSF according to the existing literature. The targets of tiapride are relatively single, while the targets of JA are more. Second, tiapride as a benzamide with low antipsychotic action, a study found 27.1% TS patients had mild or moderate adverse effects including dizziness, nausea, and dry mouth (Fekete et al. 2021). While no obvious adverse events of JA were observed in our previous study.

The present study had some limitations. First, JA is a compound prescription formulation; therefore, the mechanism of

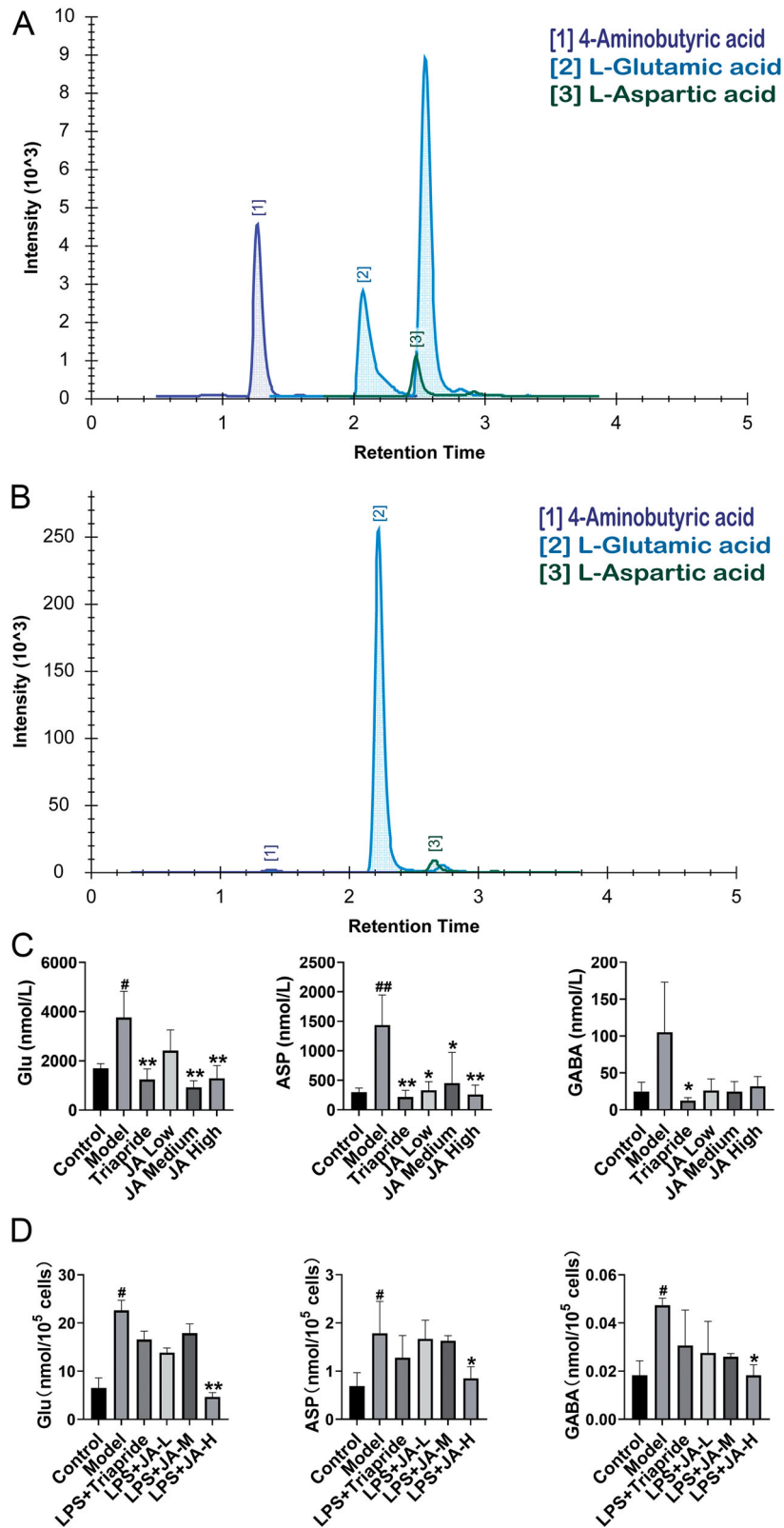


**Figure 8.** Chromatogram for GABA, Glu, and ASP in (A) CSF and (B) BV2 cells. The levels of amino acid neurotransmitters in (C) CSF and (D) BV2 cells. Data are presented as mean  $\pm$  SD. # and ## indicate  $p < 0.05$  and  $p < 0.01$ , respectively, when data are compared to those for the control group. \* and \*\* indicate  $p < 0.05$  and  $p < 0.01$ , respectively, when data are compared to those for the model group.

action and pharmacokinetic properties of each herb must be verified. Additionally, the study was mainly focused on NMDAR1; consequently, the roles of other GluRs are unclear.

## Conclusions

The present study showed that JA was effective in alleviating the severity of stereotyped behaviour and improving the classification stereotyped behaviour in rats with TS. Moreover, JA decreased the levels of Glu, ASP, and GABA. It also inhibited microglia activation and regulated the NMDAR/MAPK/CREB signaling pathway in TS *in vitro* and *in vivo*. Our data show that JA may be a promising therapeutic agent for the clinical treatment of TS, which provides a basis for perfecting studies on the mechanism of action of JA in the treatment of TS.

## Disclosure statement

No potential conflict of interest was reported by the author(s).

## Funding

This research was supported by the National Natural Science Foundation of China under Grant [81774364 and 82174435].

## References

- Aida T, Yoshida J, Nomura M, Tanimura A, Iino Y, Soma M, Bai N, Ito Y, Cui W, Aizawa H, et al. 2015. Astroglial glutamate transporter deficiency increases synaptic excitability and leads to pathological repetitive behaviors in mice. *Neuropsychopharmacology*. 40(7):1569–1579.
- Albin RL, Mink JW. 2006. Recent advances in Tourette syndrome research. *Trends Neurosci*. 29(3):175–182.
- Arcuri C, Mecca C, Bianchi R, Giambanco I, Donato R. 2017. The pathophysiological role of microglia in dynamic surveillance, phagocytosis and structural remodeling of the developing CNS. *Front Mol Neurosci*. 10: 191–213.
- Beppu K, Kosai Y, Kido MA, Akimoto N, Mori Y, Kojima Y, Fujita K, Okuno Y, Yamakawa Y, Ifuku M, et al. 2013. Expression, subunit composition, and function of AMPA-type glutamate receptors are changed in activated microglia; possible contribution of GluA2 (GluR-B)-deficiency under pathological conditions. *Glia*. 61(6):881–891.
- Byrnes KR, Stoica B, Loane DJ, Riccio A, Davis MI, Faden AI. 2009. Metabotropic glutamate receptor 5 activation inhibits microglial associated inflammation and neurotoxicity. *Glia*. 57(5):550–560.
- Chang Y, Lee JJ, Hsieh CY, Hsiao G, Chou DS, Sheu JR. 2009. Inhibitory effects of ketamine on lipopolysaccharide-induced microglial activation. *Mediators Inflamm*. 2009:705379.
- Che F, Zhang Y, Wang G, Heng X, Liu S, Du Y. 2015. The role of GRIN2B in Tourette syndrome: results from a transmission disequilibrium study. *J Affect Disord*. 187:62–65.
- Chen J, Leong PK, Leung HY, Chan WM, Li Z, Qiu J, Ko KM, Chen J. 2019. A Chinese herbal formulation, Xiao-Er-An-Shen decoction, attenuates Tourette syndrome, possibly by reversing abnormal changes in neurotransmitter levels and enhancing antioxidant status in mouse brain. *Front Pharmacol*. 10:812.
- Fekete S, Egberts K, Preissler T, Wewetzer C, Mehler-Wex C, Romanos M, Gerlach M. 2021. Estimation of a preliminary therapeutic reference range for children and adolescents with tic disorders treated with tiapride. *Eur J Clin Pharmacol*. 77(2):163–170.
- Haddad JJ. 2005. N-Methyl-D-aspartate (NMDA) and the regulation of mitogen-activated protein kinase (MAPK) signaling pathways: a revolving neurochemical axis for therapeutic intervention? *Prog Neurobiol*. 77(4): 252–282.
- Ishiguro T, Sakata-Haga H, Fukui Y. 2016. A 5-HT<sub>2A/2C</sub> receptor agonist, 1-(2,5-dimethoxy-4-iodophenyl)-2-aminopropane, mitigates developmental neurotoxicity of ethanol to serotonergic neurons. *Congenit Anom (Kyoto)*. 56(4):163–171.
- Kanaan AS, Gerasch S, Garcia-Garcia I, Lampe L, Pampel A, Anwender A, Near J, Moller HE, Muller-Vahl K. 2017. Pathological glutamatergic neurotransmission in Gilles de la Tourette syndrome. *Brain*. 140(1): 218–234.
- Koga Y, Tsurumaki H, Aoki-Saito H, Sato M, Yatomi M, Takehara K, Hisada T. 2019. Roles of cyclic AMP response element binding activation in the ERK1/2 and p38 MAPK signaling pathway in central nervous system, cardiovascular system, osteoclast differentiation and mucin and cytokine production. *IJMS*. 20(6):1346.
- Kumar A, Williams MT, Chugani HT. 2015. Evaluation of basal ganglia and thalamic inflammation in children with pediatric autoimmune neuropsychiatric disorders associated with streptococcal infection and Tourette syndrome: a positron emission tomographic (PET) study using <sup>11</sup>C-[R]-PK11195. *J Child Neurol*. 30(6):749–756.
- Lenington JB, Coppola G, Kataoka-Sasaki Y, Fernandez TV, Palejev D, Li Y, Huttner A, Pletikos M, Sestan N, Leckman JF, et al. 2016. Transcriptome analysis of the human striatum in Tourette syndrome. *Biol Psychiatry*. 79(5):372–382.
- Long H, Ruan J, Zhang M, Wang C, Huang Y. 2019a. Gastrodin alleviates Tourette syndrome via Nrf-2/HO-1/HMGB1/NF- $\kappa$ B pathway. *J Biochem Mol Toxicol*. 33(10):e22389.
- Long H, Wang C, Ruan J, Zhang M, Huang Y. 2019b. Gastrodin attenuates neuroinflammation in DOI-induced Tourette syndrome in rats. *J Biochem Mol Toxicol*. 33(5):e22302.
- Mahone EM, Puts NA, Edden RAE, Ryan M, Singer HS. 2018. GABA and glutamate in children with Tourette syndrome: A (1)H MR spectroscopy study at 7T. *Psychiatry Res Neuroimaging*. 273:46–53.
- Murugan M, Ling EA, Kaur C. 2013. Glutamate receptors in microglia. *CNS Neurol Disord Drug Targets*. 12(6):773–784.
- Murugan M, Sivakumar V, Lu J, Ling EA, Kaur C. 2011. Expression of N-methyl D-aspartate receptor subunits in amoeboid microglia mediates production of nitric oxide via NF- $\kappa$ B signaling pathway and oligodendrocyte cell death in hypoxic postnatal rats. *Glia*. 59(4):521–539.
- O'Brien KB, Sharrief AZ, Nordstrom EJ, Travanty AJ, Huynh M, Romero MP, Bittner KC, Bowser MT, Burton FH. 2018. Biochemical markers of striatal desensitization in cortical-limbic hyperglutamatergic TS- & OCD-like transgenic mice. *J Chem Neuroanat*. 89:11–20.
- Puts NA, Harris AD, Crocetti D, Nettles C, Singer HS, Tommerdahl M, Edden RA, Mostofsky SH. 2015. Reduced GABAergic inhibition and abnormal sensory symptoms in children with Tourette syndrome. *J Neurophysiol*. 114(2):808–817.
- Rapanelli M, Frick L, Jindachomthong K, Xu J, Ohtsu H, Nairn AC, Pittenger C. 2018. Striatal signaling regulated by the H3R histamine receptor in a mouse model of tic pathophysiology. *Neuroscience*. 392:172–179.
- Rapanelli M, Frick LR, Pogorelov V, Ota KT, Abbasi E, Ohtsu H, Pittenger C. 2014. Dysregulated intracellular signaling in the striatum in a pathophysiologically grounded model of Tourette syndrome. *Eur Neuropsychopharmacol*. 24(12):1896–1906.
- Robertson MM. 2008a. The prevalence and epidemiology of Gilles de la Tourette syndrome. Part 1: the epidemiological and prevalence studies. *J Psychosom Res*. 65(5):461–472.
- Robertson MM. 2008b. The prevalence and epidemiology of Gilles de la Tourette syndrome. Part 2: Tentative explanations for differing prevalence figures in GTS, including the possible effects of psychopathology, aetiology, cultural differences, and differing phenotypes. *J Psychosom Res*. 65(5):473–486.
- Szejko N, Lombroso A, Bloch MH, Landeros-Weisenberger A, Leckman JF. 2020. Refractory Gilles de la Tourette Syndrome-many pieces that define the puzzle. *Front Neurol*. 11:589511.
- Takeuchi H, Suzumura A. 2014. Gap junctions and hemichannels composed of connexins: potential therapeutic targets for neurodegenerative diseases. *Front Cell Neurosci*. 8:189.
- Thomas DM, Kuhn DM. 2005. MK-801 and dextromethorphan block microglial activation and protect against methamphetamine-induced neurotoxicity. *Brain Res*. 1050(1–2):190–198.
- Zhang W, Yu W, Liu X, Wang Q, Bai X, Cui X, Wang S. 2020. Effect of Jian-Pi-Zhi-Dong Decoction on the amino acid neurotransmitters in a rat model of Tourette syndrome and comorbid anxiety disorder. *Front Psychiatry*. 11:515.